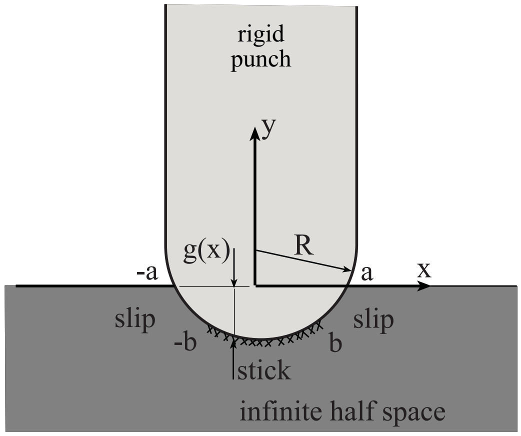

Figure 1. Rigid punch on elastic half plane.

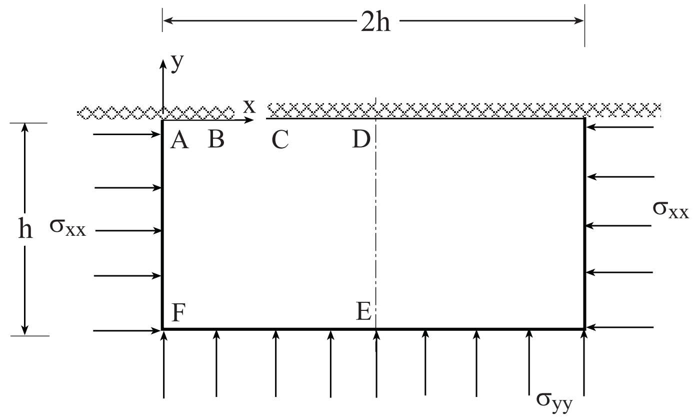

Figure 2. Two-dimensional linear elastic slab compressed by a rigid plate.

friction, and σ_{yy} is the normal stress in the y-direction. No difference in f is assumed for static and kinematic friction. The parameter $s = \pm 1$ is chosen so that the direction of the shear stress in the contact area coincides with that of the tangential shift $\text{sgn}(\Delta U) = \text{sgn}(\tau_{xy})$. Note that $g(x)$ is calculated from the displacement of the rigid body Δ and its shape. It is assumed that $g(x)$ and, hence, the contact zone are small compared with other geometrical parameters of the problem. Thus, along the contact zone, $V(x) \approx -U_r(\theta)$ where $U_r(\theta)$ is the displacement in the radial direction; $\tau_{xy}(x) \approx \tau_{r\theta}(\theta)$ and $\sigma_{yy}(x) \approx \sigma_{rr}(\theta)$.

In the stick region for stationary, receding and advancing contact without friction, the boundary conditions are given by

$$V(x) = g(x) \tag{3}$$

$$U(x) = 0 \tag{4}$$

where $U(x)$ is the displacement in the x-direction. Here, $U(x) \approx U_\theta(\theta)$. For the problems solved in which contact is along straight surfaces, the solution is exact. For advancing contact in the presence of friction, eq. (4) is replaced by

$$\frac{\partial U}{\partial \Delta} = 0 \,. \tag{5}$$

In the problems studied here, the punch is lowered by a displacement Δ. The force resulting from the applied displacement is calculated by integrating the normal stress between the rigid punch and the elastic surface, as well as at the lower end of the elastic body (half-space).

3 Frictional contact between a linear, elastic slab and a rigid plate

The problem of a two-dimensional linear, elastic slab compressed against a rigid plate shown in Fig. 2 is considered. This example has the advantage of having three different contact conditions, namely, stick, slip and free surface. Using the BEM and FEM, this problem was solved in [22]. Reasonable agreement was achieved with these two numerical techniques.

The same material and geometric properties used in [22] are employed here; namely, Young's modulus is $E = 13$ GPa, Poisson's ratio $\nu = 0.2$ and the height $h = 40$ mm. Plane strain conditions are imposed in this problem, as well as all other problems studied here. As a result of symmetry, only one-half of the slab is modeled. The traction boundary conditions are given by $\sigma_{xx} = -10$ MPa along FA and $\sigma_{yy} = -5$ MPa along FE. Symmetry conditions are applied along DE as $U(x = h, y) = 0$ and $\partial V(x = h, y)/\partial x = 0$.

The contact algorithm is applied along the contact area AD. Since the slab is not in contact with the rigid plate along AB, free surface conditions are applied. Along BC there is slip between the slab and the plate; while along CD, the slab sticks to the plate. The effect of five friction coefficients ($f = 0, 0.4, 0.8, 1.0$ and 1.3) on the length of the three contact zones is studied. Comparison is made to the results obtained in [22] for $f = 1$.

A dense FD mesh consisting of 200 points in the x-direction and 100 points in the y-direction is constructed for the square ADEF in Fig. 2. The physical domain is mapped into the numerical domain ($1 \le \xi \le 2$ and $1 \le \eta \le 2$) using a fourth order polynomial for x as

$$x = \sum_{n=0}^{4} a_n \xi^n \tag{6}$$

and a second order polynomial for y

$$y = \sum_{m=0}^{2} b_m \eta^m \,. \tag{7}$$

This technique is described in [12]. The coefficients a_n, $n = 0 \ldots 4$ and b_m, $m = 0 \ldots 2$ are given in Table 1. They are chosen by trial and error so that the derivatives of x and y in eqs. (6)